Quantum mechanical studies of 2D nanobiohybrids (Review Article)

Cite as: Low Temp. Phys. **48**, 278 (2022); https://doi.org/10.1063/10.0009731
Submitted: 18 February 2022 • Published Online: 12 April 2022

S. G. Stepanian and L. Adamowicz

Low Temperature Physics ARTICLE scitation.org/journal/ltp

Quantum mechanical studies of 2D nanobiohybrids (Review Article)

Cite as: Fiz. Nizk. Temp. **48**, 315–323 (April 2022); doi: 10.1063/10.0009731
Submitted: 18 February 2022

S. G. Stepanian[1,a)] and L. Adamowicz[2]

AFFILIATIONS

[1]B. Verkin Institute for Low Temperature Physics and Engineering of the National Academy of Sciences of Ukraine, Kharkiv 61103, Ukraine
[2]Department of Chemistry and Biochemistry, University of Arizona, Tucson AZ 85721, USA Interdisciplinary Center for Modern Technologies, Nicolaus Copernicus University, Toruń PL 87-100, Poland

[a)]**E-mail:** stepanian@ilt.kharkov.ua

ABSTRACT

We considered the recent application of quantum mechanical methods for studying the structure, interaction energies, as well as vibrational and electronic spectra of complexes of 2D nanomaterials (graphene, graphene oxide) with biological molecules. We analyzed how to overcome the main problems arising in computational studies of 2D nanobiohybrids, namely, the large size of systems, the nonuniformity of 2D nanomaterials, the need to use methods that can correctly take into account dispersion interactions. An analysis of the results of quantum mechanical studies, published over the recent decade, showed that the development of theoretical calculation methods and a significant increase in the productivity of computing technology made it possible to calculate not only the structure and interaction energies of nanobiosystems, but also their vibrational and electronic spectra.

Contents

1. INTRODUCTION

In the recent decade, 2D nanomaterials have been in the focus of attention of many researchers due to their unique characteristics, which determine the wide possibilities of their practical use.[1–8] The thickness of 2D nanomaterials is from one to several atomic layers (Fig. 1), which provides a uniquely high ratio of their surface area and volume. Studies of the structure, spectral, electronic, and mechanical properties of 2D nanomaterials and their complexes are carried out using practically all modern experimental methods. In addition, methods of quantum mechanical calculations are actively used to study the properties of 2D nanomaterials. The computational studies of the interactions between 2D nanomaterials and various guest molecules provide important information about the noncovalent interactions and thus can guide the development of devices which are based on the 2D nanomaterials.

In 2015 we summarized the current results of quantum mechanical researches in the field of theoretical modeling of noncovalent functionalization of carbon materials (nanotubes and graphene).[9] We demonstrated that significant progress in this field had been achieved due to two factors: the development of new effective quantum chemical methods which are capable of accurately describing the system stabilized by dispersion interactions and due to continuously increasing power of modern computers and the development of efficient algorithms for the use of multiprocessor computer clusters.[9] In subsequent years there has been a significant increase in the number of published articles on various aspects of the interactions in 2D nanomaterials with biological

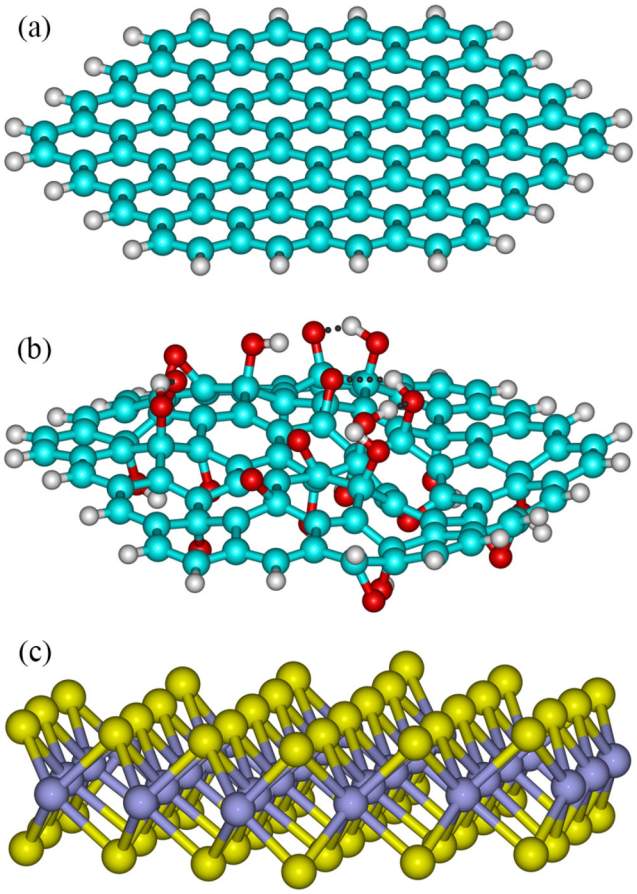

FIG. 1. Schematic representations of some 2D nanomaterials: graphene (a), graphene oxide (b), MoS_2 (c).

molecules. In this review, we considered recent results of quantum mechanical modeling of systems formed by 2D nanomaterials and biomolecules. The main attention was paid to graphene oxide and molybdenum disulfide complexes, which are the most frequent objects of computational researches. We considered the main problems that arise in these studies. Among them, it is necessary to note the significant size of the simulated systems, the need to use computational methods capable of correctly describing dispersion interactions, and the heterogeneity of the structure of nanomaterials. It should be noted that most of the theoretical studies are devoted to calculations of the structure and interaction energies in complexes of 2D nanomaterials with biomolecules. However, in recent years, more researches have also been devoted to the calculation of the electronic and vibrational spectra of such systems.

An analysis of the results of computational studies of complexes formed by 2D nanostructures showed that at present the main problem of these studies is the choice of suitable models of nanostructures that correspond as closely as possible to real systems in experimental studies. The first, in most cases, calculations are performed for nanomaterials with an ideal unperturbed structure. At the same time, the structure of real nanomaterials has a significant number of different defects. These defects affect both the properties of the nanomaterials themselves and their interactions with guest molecules. Another problem is the need to take into account the influence of the environment on the characteristics of nanocomplexes. This is especially important when modeling the interaction of 2D nanomaterials with biomolecules. In most cases, experimental studies of such systems are carried out in aqueous solutions. As a result, it is difficult to directly compare the results of the calculation for too simple model systems with experimental data. This is especially important for the interaction energies that are calculated in most theoretical studies. In this case the polar environment can have a significant effect on the calculated energies. In general, the use of quantum mechanical methods for calculating the various characteristics of the 2D nanomaterial complexes can provide an understanding of the mechanisms for the formation and stabilization of nanobiocomplexes.

2. COMPUTATIONAL METHODS

In this section, we briefly discuss the ability of different computational approaches to correctly predict the structures, interaction energies as well as vibrational and electronic spectra of noncovalent complexes of 2D nanomaterials. The second-order many-body perturbation theory (MP2[10] is the minimal *ab initio* level of theory which is able to account for the main part of the dispersion energy. The significant disadvantage of this method is its high computational cost, which limits its use in studies of complexes involving 2D nanomaterials. Post-MP2 methods are much more computationally damaging than MP2 and cannot be applied to study large. The Density Functional Theory (DFT) method is an effective alternative to the MP2 method. The inability of the DFT method to correctly account for the long-range dispersion interaction was the main drawback of the method for a long time.[11,12]

At the present time, two approaches are used to allow the DFT method to handle the dispersion interactions in noncovalently bonded systems. The first approach is the dispersion-corrected DFT (DFT-D). Several schemes of this type include the D2 version of Grimme's dispersion method,[13] the D3 version of Grimme's dispersion method with the original D3 damping function,[14] and the D3 version of Grimme's dispersion method with the Becke–Johnson damping.[15] Another approach is the new-generation density functionals, which overcome this deficiency. These are density functionals MPWB1K,[16] MPW1B95[16] as well as Minnesota family of functionals: M05-2X,[17] M06-2X,[18] M11,[19] N12-SX,[20] MN12-SX,[20] and MN-15.[21]

TABLE I. Interaction energies (*IE*, kJ/mol) calculated for *Conformation A* of the SWNT-cytosine dimer at the MP2 level of theory with different basis sets for the geometry of the complex obtained in a BSSE-free optimization at the MP2/BS1 level.[22]

Method/basis set (SWNT) | basis set (cytosine)	*IE* (MP2)
MP2/6-31G(d) | 6-31++G(d,p)	−50.3
MP2/6-31 + G(d) | 6-31++G(d,p)	−52.4
MP2/6-311 + G(d) | 6-311++G(d,p)	−60.7
MP2/6-311 + G(2d) | 6-311++G(2d,p)	−62.4

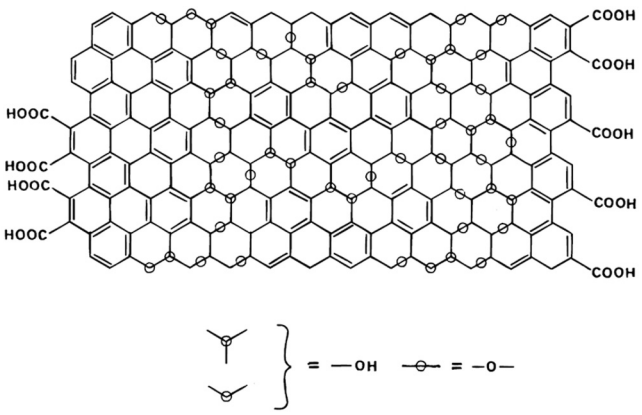

FIG. 2. Structural model of GO.[28]

Various basis sets were used in the calculations of the noncovalent interactions of complexes with 2D nanomaterials. The performance of several standard basis sets in the range from the 6-31G(d) basis to the 6-311++G(2d,p) basis was tested at the MP2 level of theory in the calculations of the cytosine-zigzag (10,0) SWCNT system[22] (Table I). As expected, the increase of the basis set led to an increase of the interaction energy. The augmentation of the basis sets of the nanotube carbon atoms with diffuse functions changed the interaction energy from −50.3 [basis set 6-31G(d)] to −52.4 kJ/mol [basis set 6-31 + G(d)]. Extending the basis set to the triple-zeta split-valence level [basis set 6-311 + G(d)] resulted in an increase of the interaction energy to −60.7 kJ/mol. The highest interaction energy of −62.4 kJ/mol was obtained with the 6-311++G(2d,p) basis set. This clearly demonstrated the importance of using high-quality basis sets in predicting the interaction energies in complexes involving 2D nanomaterials.[22] Basis sets with the effective core potential (ECP) are usually used in the calculations of transition metals dichalcogenides. The most commonly used basic sets are the LanL2DZ ECP, LanL2DZdp[23–26] and Stuttgart RSC 1997 ECP.[27]

3. COMPLEXES OF GRAPHENE OXIDE WITH BIOMOLECULES

3.1. Structure of graphene oxide

Graphene oxide (GO) is a single layer of graphite oxide and can be produced using different chemical methods. The first realistic model of GO was proposed by Lerf *et al.*[28] and He *et al.*[29] (Lerf–Klinowski model). They demonstrated that the main functional groups on graphene oxide are epoxy (1,2-ether) and hydroxyl groups (Fig. 2), with some hydroxyl, carbonyl, and carboxyl groups at the edge. Based on the experimental results, the authors suggested that graphene oxide might contain aromatic "islands" of variable size which have not been oxidized.

The optimal arrangement of oxygen-containing groups on the GO surface was established using calculations of various GO structures performed at the DFT/B3LYP/ 6-31++G(d,p) level of theory (Fig. 3). The results of these calculations showed that GO structures with a compact arrangement of oxygen-containing groups (structures D and E) are the more stable. It should be noted that the structure in which oxygen-containing groups are located at the edge of the GO fragment is the most stable one (structure D). At the same time, structures in which oxygen-containing groups are evenly distributed on the GO surface have much higher relative energies and, respectively, lower stabilities. This allows us to conclude that the most energetically stable forms of weakly oxidized or reduced GO with a low content of oxygen-containing groups should include significant zones with an unperturbed sp^2 carbon surface. This is important since the presence of such zones may allow the formation of stacking complexes of the carbon surface

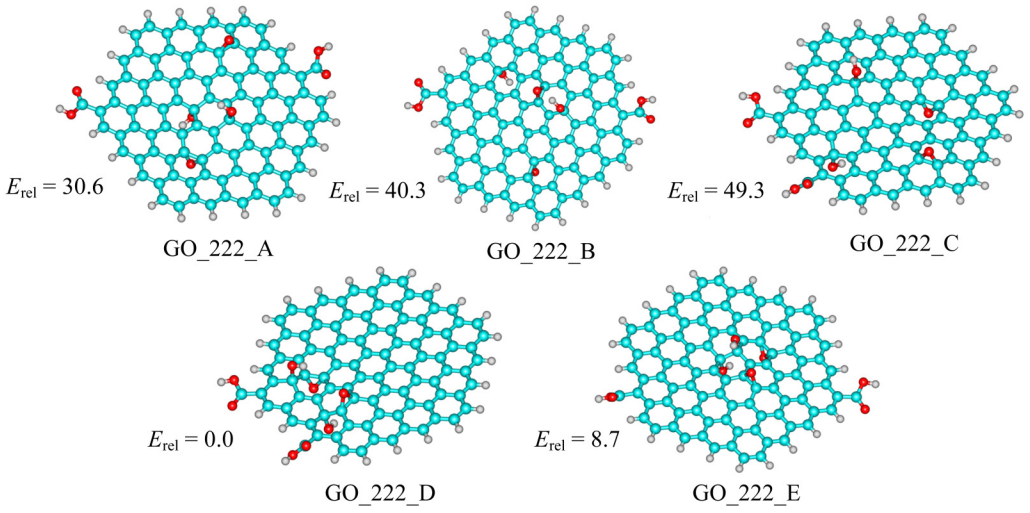

FIG. 3. Structure and relative energies E_{rel} (kcal/mol) of different GO models [B3LYP/6-31++G(d,p)].

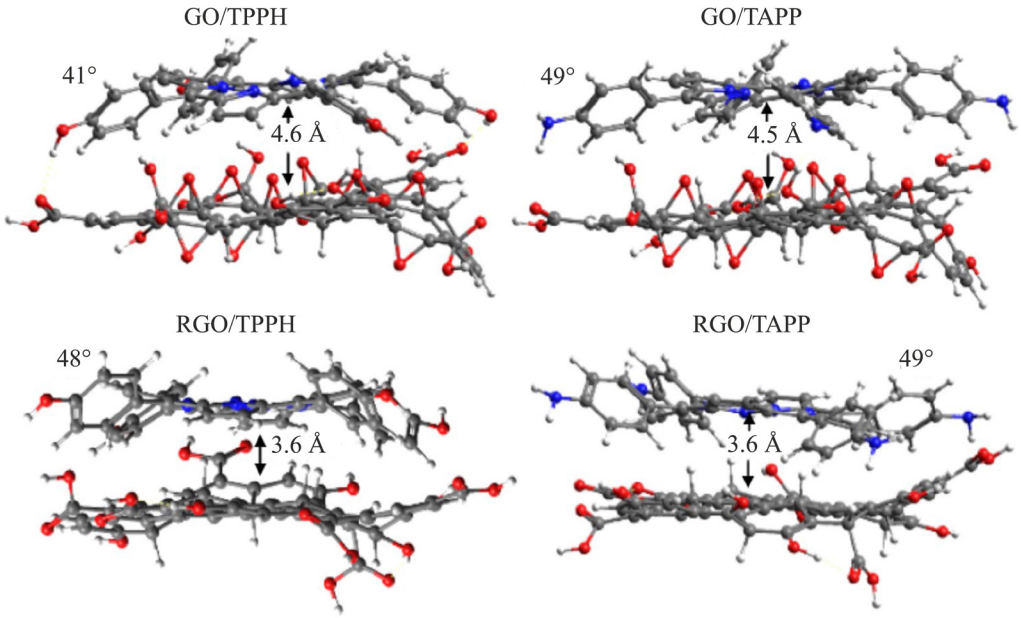

FIG. 4. Geometries of the optimized nanohybrids. Highlighted are the distance between porphyrin and GO/RGO planes as well as the dihedral angle that describes the porphyrins' phenyl ring out-of-plane rotation.[34]

with π-conjugated molecules. Moreover, such complexes can be additionally stabilized due to the formation of hydrogen bonds between guest molecules and oxygen-containing groups. Yan and Chou reported a detailed study of the oxidation functional groups on graphene based on density-functional calculations.[30] They investigated the effects of single functional groups and their various combinations on the electronic and structural properties and demonstrated that epoxy and hydroxyl groups tend to aggregate on the graphene plane.

3.2. Complexes of graphene oxide with porphyrine derivatives

2D nanomaterial complexes with porphyrin derivatives attract considerable attention due to their distinct electronic properties that have enabled a wide spectrum of light-mediated applications including optoelectronics, fabrication of novel photo-voltaic cells, the use in photodynamic therapy.[31–33] Porphyrins possess an extended π-conjugated system and are characterized by remarkably high extinction coefficients in the visible spectral region. The structure and electronic spectra of graphene and GO complexes with neutral and charged porphyrin derivatives were actively studied using quantum mechanical methods.

Siklitskaya *et al.* studied hybrids of GO and RGO with two metal-free porphyrins (5,10,15,20-tetrakis(4-aminophenyl) porphyrin (TAPP) and 5,10,15,20-tetrakis[4-hydroxyphenyl) porphyrin (TPPH)] using the BP86 density functional supplemented with D3BJ dispersion correction.[34] Optimized structural models of the nanohybrids are shown in Fig. 4. It was demonstrated that the presence of GO or reduced GO influenced both porphyrins in a similar way, i.e., the molecules become more planar as indicated by the decrease of the dihedral angle describing out-of-plane tilt of the phenyl rings. It is about 60° for the isolated porphyrins while it ranges between 41° and 49° in the case of the nanohybrid. Complexes that involved reduced GO model featured porphyrin rings on average 1 Å closer to the graphene plane than in the case of the GO species. Calculated binding energies are presented in Table II. Decomposition of the energies demonstrated significant deformation energies both for GO and the porphyrine derivatives. Comparison of the experimental and computed UV–Vis absorption spectra is shown in Fig. 5. Experimental absorption spectra feature a common maximum at about 450 nm. The experimental Soret band shifts upon porphyrin adsorption on GO/RGO sheet are well reproduced in the calculations.

The noncovalent interaction of neutral meso-5,10,15, 20-tetraphenyl porphyrin (TPP), as well as of porphyrin core (porphin molecule), with graphene, was studied using the M05-2X/6-31G(d)

TABLE II. Binding energy (E bind) released upon nanohybrid formation and its decomposition. All values are in kcal/mol.[34]

Nanohybrid	*E* bind	*E* graphene deform	*E* porph deform	*E* int
GO/TPPH	−21.2	14.9	13.9	−50.0
GO/TAPP	−24.4	18.4	7.3	−50.1
RGO/TPPH	−36.2	10.1	9.2	−55.5
RGO/TAPP	−36.7	8.5	5.9	−51.1

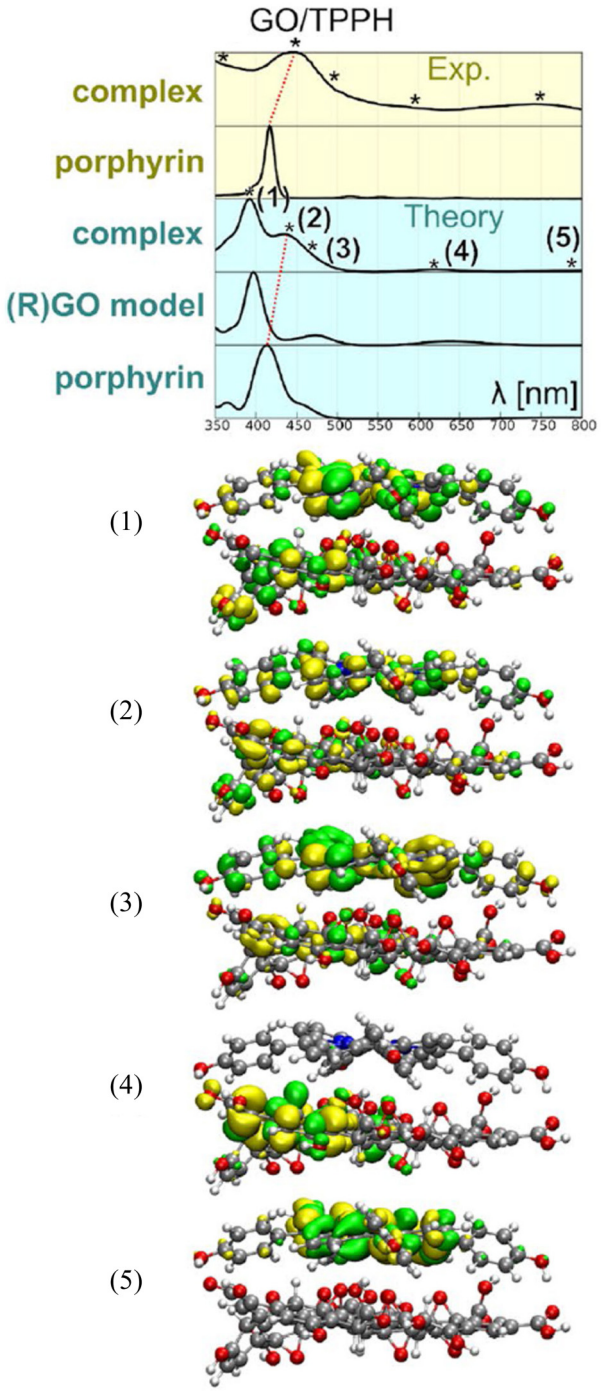

FIG. 5. Top: comparison of experimental (yellow background) and computed (cyan background) absorption spectra. The spectra plotted are from the top: nanohybrid (exp), porphyrin (exp), nanohybrid (theory), graphene species (theory), and porphyrin (theory). Red dotted line guides identification of Soretband shift in theory and experiment. Bottom: isosurface plots of transition densities for key electronic excitations (1)–(5).[34]

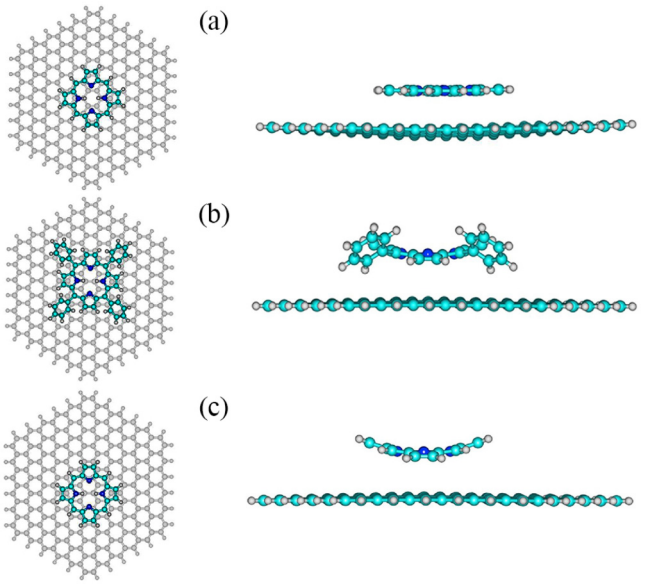

FIG. 6. Calculated [M05-2X/6-31G(d)] structures of the Gr-porphin (a), Gr-TPP (b), and graphene-porphyrin core of TPP (c) complexes (top and side views).[35]

method.[35] It was shown that the π-π-stacking interaction of the porphyrin core with graphene provides the main contribution to the interaction energy. It was also found that in the TPP structure, due to a steric hindrance, the peripheral rings arranged around the porphyrin core are not coplanar with the core. This arrangement prevents the core from approaching the graphene surface at a distance similar as for the porphin molecule. The interaction of TPP with graphene leads to distortion of the flat structure of the porphyrin core and to some twisting of its side rings, so the dihedral angles between the plane of the

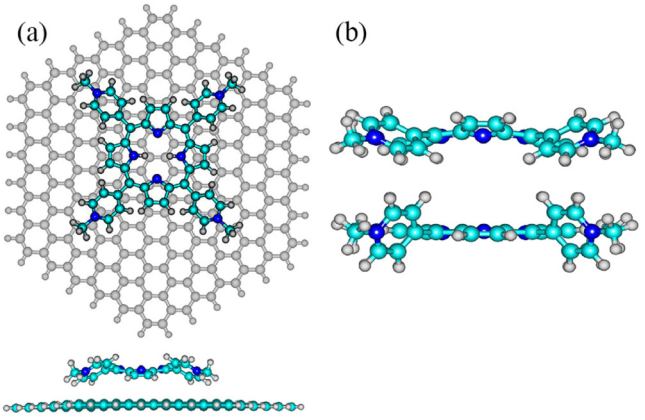

FIG. 7. Calculated structure of the TMPyP4-Gr complex (top view and side view) (a). A comparison of the structure of the TMPyP4 molecule in the complex (top) and the single TMPyP4 molecule (b).[36]

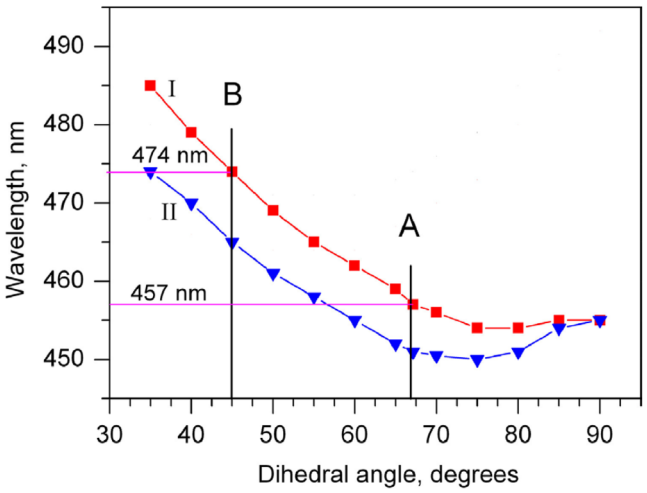

FIG. 8. Dependency of the Soret band wavelengths on the rotation of the methylpyridinium rings relative to the plane of the TMPyP4 porphyrin core calculated at the TD-B3LYP [PCM(water)]/6-31 + G(d) level of theory. Geometry of the fully optimized isolated TMPyP4 molecule (A); side residues are rotated to match the positions of the residues in the TMPyP4-graphene complex (B). All other structural parameters are optimized.[36]

porphyrin core and the planes of the side residues decrease (Fig. 6). Thus, a flattening of the TPP structure upon adsorption on graphene occurs.

The M05-2X/6-31G(d) level of theory was used to investigate the structural and spectral transformations of cationic meso-5,10,15,20-tetra-(N-methyl-4-pyridyl) porphyrin (TMPyP4) at adsorption on graphene.[36] It was shown that the binding of TMPyP4 with graphene is stronger as compared to the neutral porphyrin (TPP) with a similar structure (−111.0 vs −22.6 kcal/mol). This is due to a large contribution from the cation-π-electrons interaction. The interaction of TMPyP4 with graphene is accompanied by a distortion of the flat structure of the porphyrin core and twisting of the side rings (Fig. 7). As a result, the porphyrin molecule flattens.

TABLE III. Electronic transitions of the TMPyP4 molecule corresponding to the Soret band (the PCM (solvent = water) TD B3LYP/6-31 + G(d) level of theory is used).[36]

System	Wavelength (shift), nm	
TMPyP4 single molecule (fully optimized geometry)	457	451
Complex TMPyP4-Gr	482 (+27)	477 (+26)
TMPyP4 (geometry as in complex with graphene)	472 (+15)	464 (+13)
TMPyP4 (MPYR residues are rotated as in the complex and fixed, other parameters are optimized)	474	465

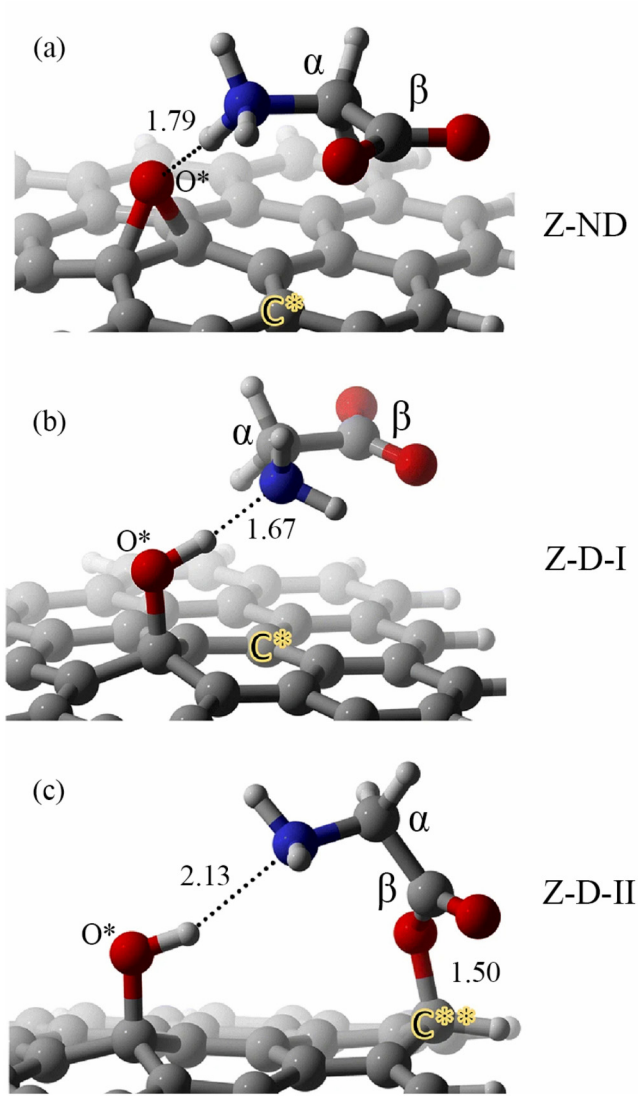

FIG. 9. Optimized geometries obtained for neutral Gly adsorbed on GO exposing an epoxy group in the gas phase. (a) Non-dissociated mode (Z-ND). (b) Dissociated mode I (Z-D-I). (c) Dissociated mode II (Z-D-II). Bond distances are given in A. C* designates the C atom of GO, nearest to Ca; C** is the carbon atom of GO nearest to an atom of the Gly conformer. O* is the O atom of epoxy/hydroxyl group on GO surface.[37]

The cationic porphyrin adsorbed to graphene induces a stronger molecule flattening in comparison with the neutral porphyrin.

TD-DFT calculatiobs [B3LYP(PCM)/6-31 + G(d)] were performed to separate the contribution of the change in the structure of the TMPyP4 molecule and the contribution from the interaction of the π-electron systems (TMPyP4 and graphene) to the shift of the two TMPyP4 Soret bands. For an isolated TMPyP4 molecule the dependency of the wavelengths of the Soret bands on the rotation of the MPYR rings was calculated In the calculations, the

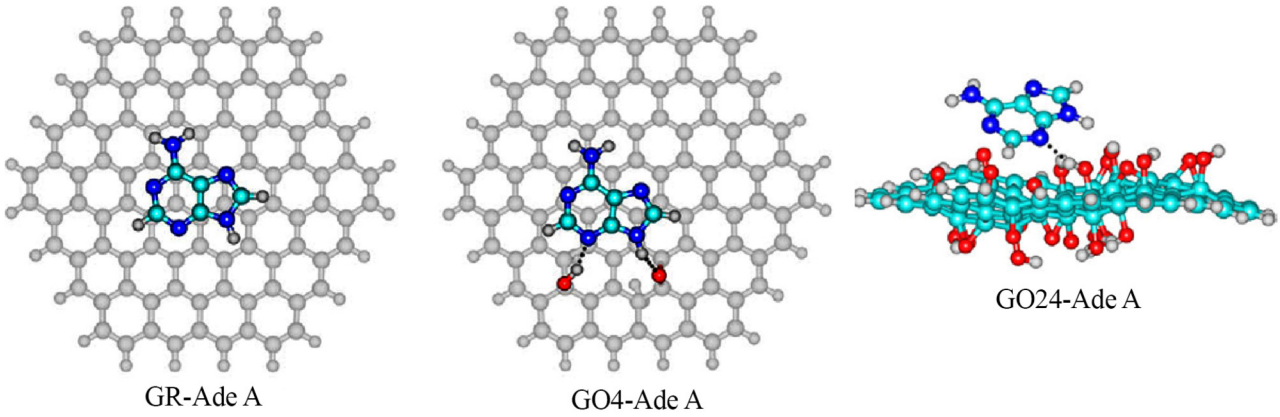

FIG. 10. The lowest energy structures of graphene-adenine (GR-Ade A) and graphene oxide-adenine complexes. Graphene oxides have 4 (GO4-Ade A) and 24 (GO24-Ade A) oxygen-containing groups, respectively.[39]

dihedral angles corresponding to the rotation of the TMPyP4 side residues were scanned from 35° to 90° while all other internal coordinates are fully optimized. The results of the calculations are presented in Fig. 8 and Table III.

As it is seen, the calculations predicted long-wavelength shifts of the two Soret bands of the TMPyP4 molecule upon the formation of a complex with graphene. The wavelengths change by +27 and +26 nm, respectively. This agrees well with the experimentally recorded Soret band shift of +28 nm. The results of the calculations also show that the main contribution to the change of the position of the Soret band comes from the deformation of the structure of the TMPyP4 molecule (+15 and +13 nm for the two transitions, respectively). Additionally, a shift of about 12 nm occurs due to the staking interaction of the π-systems of bonds of the TMPyP4 molecule and graphene.[36] It was also demonstrated that the TMPyP4 molecule creates an area of negative potential in graphene close to the porphyrin adsorption site.

3.3. Interaction of graphene oxide with aminoacids

Rossi-Fernández *et al.* investigated interactions between GO and zwitterionic form of aminoacid glycine.[37] Structure of the GO-glycine complex (Fig. 9) was calculated at the B3LYP(GD3BJ)/6-311++G(d,p) level of theory. The nondissociative adsorption modes for zwitterionic and neutral Gly conformers interacting with an epoxy group of GO showed binding energies of 12.2 and 14.4 kcal/mol. The adsorption of glycine onto the GO surface was highly dominated by noncovalent interactions.

3.4. Physisobrption of nucleic acid bases on graphene oxide

Structure, interaction energies, and vibrational spectra of the GO-cytosine[38] and GO-adenine[39] complexes were calculated at the B3LYP(GD3BJ)/6-31++G(d,p) level of theory. The calculations demonstrated that the binding energy of adenine

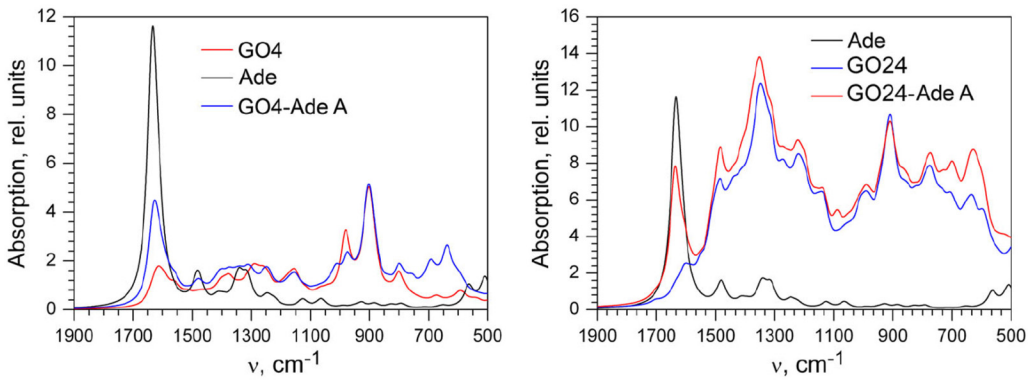

FIG. 11. Fingerprint region of the calculated IR spectra of the GO4-Ade A and GO24-Ade A complexes. Frequencies are scaled down by a uniform factor of 0.98. Bands are approximated by 40 cm^{-1} full-width-at-half-maximum Lorentzian lineshapes.[39]

stacking with graphene depends on the structure of the carbon surface and has a value about −20 kcal/mol in vacuum. The adenine-GO4 interaction occurs due to the p-p stacking and H-bonding with the GO oxygen-containing groups of GO4 (Fig. 10). In all conformations, the adenine molecule interacts more strongly with GO4 than with pristine graphene (−27 vs −20 kcal/mol). The calculations demonstrate that the contribution of the H-bonding to the total energy of the interaction between adenine and GO reaches 35–40%. It is shown that the addition of a large number of oxygen-containing groups to GO leads to a significant distortion of the planar structure of graphene. The orientation of the adenine molecule on the strongly oxidized graphene (O:C = 24:96, GO24) is determined by a network of hydrogen bonds between adenine and the oxygen-containing groups of GO. Thus, we conclude that the binding energy of adenine with nanomaterials of the graphene-family is quite strong. It is stronger for weakly oxidized graphene than for strongly oxidized graphene.

Graphic representation of the IR spectra of the most stable GO4-Ade A and GO24-Ade A complexes are shown in Fig. 11. They show significant changes in the IR spectra in the range of 1800–1400 cm^{-1}. The changes depend on the type of the H-bonding in the complex. As it is seen, the interaction of adenine with graphene oxide results in larger (as compared with the complexes of adenine with graphene) shifts of most adenine bands due to the formation of the H-bonds. In addition, there are also significant changes in the intensities of the adenine vibrations in the complexes with graphene oxide.

4. CONCLUSIONS

The presented analysis of the results of quantum mechanical calculations of 2D complexes of nanostructures with biological molecules demonstrates the ability of modern theoretical methods to predict a wide range of important parameters of nanobiocomplexes: structure, interaction energies, and spectral characteristics. In those cases where a direct comparison of the calculated characteristics with experimental results is possible, good agreement between the calculated and observed data is observed. This is especially true for the calculated electronic spectra. However, in some cases, to obtain a better agreement between the calculated and observed characteristics of nanobiocomplexes it is necessary to use more realistic models in the calculations. It can be hoped that a further increase in the power of computer systems will make this possible in the coming years.

ACKNOWLEDGMENTS

This work was supported by the National Academy of Sciences of Ukraine (under Grant No. 0120U100157). An allocation of computer time from the Computational Center at Institute for Low Temperature Physics and Engineering and from UA Research High Performance Computing (HPC) and High Throughput Computing (HTC) at the University of Arizona is gratefully acknowledged.

REFERENCES

[1]V. Georgakilas, M. Otyepka, A. B. Bourlinos, V. Chandra, N. Kim, K. C. Kemp, P. Hobza, R. Zboril, and K. S. Kim, Chem. Rev. **112**, 6156 (2012).
[2]D. Chen, H. Feng, and J. Li, Chem. Rev. **112**, 6027 (2012).
[3]A. Iwan and A. Chuchmała, Prog. Polym. Sci. **37**, 1805 (2012).
[4]M.-H. Kang, D. Lee, J. Sung, J. Kim, B. H. Kim, and J. Park, "Structure and chemistry of 2D materials," in *Comprehensive Nanoscience and Nanotechnology* (Elsevier, 2019), Vol. 2, p. 55.
[5]T. Govindaraju and M. B. Avinash, Nanoscale **4**, 6102 (2012).
[6]K. F. Mak, C. Lee, J. Hone, J. Shan, and T. F. Heinz, Phys. Rev. Lett. **105**, 136805 (2010).
[7]M. Osada and T. Sasaki, Adv. Mater. **24**, 210 (2012).
[8]W. Choi, N. Choudhary, and G. H. Han, J. Park, D. Akinwande, and Y. H. Lee, Mater. Today **20**, 116 (2017).
[9]S. G. Stepanian, M. V. Karachevtsev, and L. Adamowicz, "Quantum-Mechanical Investigations of Noncovalent Interactions of Carbon Materials," in *Nanobiophysics*: *Fundamentals and Applications*, edited by V. A. Karachevtsev (Pan Stanford Publishing Pte. Ltd., 2015), p. 1.
[10]C. Møller and M. S. Plesset, Phys. Rev. **46**, 618 (1934).
[11]A. J. Cohen, P. Mori-Sánchez, and W. Yang, Theory Chem. Rev. **112**, 289 (2012).
[12]A. Ruzsinszky and J. P. Perdew, Comp. Theor. Chem. **963**, 2 (2011).
[13]S. Grimme, J. Comp. Chem. **27**, 1787 (2006).
[14]S. Grimme, J. Antony, S. Ehrlich, and H. Krieg, J. Chem. Phys. **132**, 154104 (2010).
[15]S. Grimme, S. Ehrlich, and L. Goerigk, J. Comp. Chem. **32**, 1456 (2011).
[16]Y. Zhao and D. G. Truhlar, J. Phys. Chem. A **108**, 6908 (2004).
[17]Y. Zhao, N. E. Schultz, and D. G. Truhlar, J. Chem. Theory Comput. **2**, 364 (2006).
[18]Y. Zhao and D. G. Truhlar, Theor. Chem. Acc. **120**, 215 (2008).
[19]R. Peverati and D. G. Truhlar, J. Phys. Chem. Lett. **2**, 2810 (2011).
[20]R. Peverati and D. C. Truhlar, Phys. Chem. Chem. Phys. **14**, 16187 (2012).
[21]H. S. Yu, X. He, S. L. Li, and D. G. Truhlar, Chem. Sci. **7**, 5032 (2016).
[22]S. G. Stepanian, M. V. Karachevtsev, A. Y. Glamazda, V. A. Karachevtsev, and L. Adamowicz, Chem. Phys. Lett. **459**, 153 (2008).
[23]P. J. Hay and W. R. Wadt, J. Chem. Phys. **82**, 270 (1985).
[24]P. J. Hay and W. R. Wadt, J. Chem. Phys. **82**, 284 (1985).
[25]P. J. Hay and W. R. Wadt, J. Chem. Phys. **82**, 299 (1985).
[26]C. E. Check, T. O. Faust, J. M. Bailey, B. J. Wright, T. M. Gilbert, and L. S. Sunderlin, J. Phys. Chem. A **105**, 8111 (2001).
[27]D. Andrae, U. Häußermann, M. Dolg, H. Stoll, and H. Preuß, Theor. Chim. Acta **77**, 123 (1990).
[28]A. Lerf, H. He, M. Forster, and J. Klinowski, J. Phys. Chem. B **102**, 4477 (1998).
[29]H. He, J. Klinowski, M. Forster, and A. Lerf, Chem. Phys. Lett. **287**, 53 (1998).
[30]J.-A. Yan and M. Y. Chou, Phys. Rev. B **82**, 125403 (2010).
[31]A. R. Monteiro, M. G. P. M. S. Neves, and T. Trindade, Chem. Plus Chem. **85**, 1857 (2020).
[32]A. Gulati and R. Kakkar, Chem. Eng. Res. Des. **153**, 21 (2020).
[33]N. Tsolekile, S. Nelana, and O. S. Oluwafemi, Molecules **24**, 2669 (2019).
[34]A. Siklitskaya, E. Gacka, D. Larowska, M. Mazurkiewicz-Pawlicka, A. Malolepszy, L. Stobiński, B. Marciniak, A. Lewandowska-Andrałojć, and A. Kubas, Sci. Rep. **11**, 7977 (2021).
[35]V. A. Karachevtsev, S. G. Stepanian, M. V. Karachevtsev, and L. Adamowicz, Comput. Theor. Chem. **1133**, 1 (2018).
[36]V. A. Karachevtsev, S. G. Stepanian, M. V. Karachevtsev, V. A. Valeev, and L. Adamowicz, J. Mol. Str. **1245**, 131056 (2021).
[37]A. C. Rossi-Fernández, N. Villegas-Escobar, D. Guzmán-Angel, S. Gutiérrez-Oliva, R. M. Ferullo, N. J. Castellani, and A. Toro-Labbé, J. Mol. Mod. **26**, 33 (2020).
[38]M. V. Karachevtsev, S. G. Stepanian, A. Y. Ivanov, V. S. Leontiev, V. A. Valeev, O. S. Lytvyn, L. Adamowicz, and V. A. Karachevtsev, J. Phys. Chem. C **121**, 18221 (2017).
[39]M. V. Karachevtsev, S. G. Stepanian, V. A. Valeev, O. S. Lytvyn, L. Adamowicz, and V. A. Karachevtsev, J. Biomol. Str. Dynamics **40**, 425 (2022).